

1 Supplemental Material

2 **S1. Study Area**



3
4 **Figure S1.** Photo of Bakersfield and the South San Joaquin Valley from the NASA (Earth
5 Research ER-2 airplane at 20-km altitude. Blue-white arrows show approximate direction of
6 prevailing winds, oil fields near Bakersfield labeled. Photo courtesy Stuart Broce, Pilot, NASA
7 Armstrong Flight Research Center.

8 **S2. Platforms**

9 **S2.1. Surface – AMOG Surveyor**

10 Mobile surface *in situ* measurements using Cavity RingDown Spectroscopy (CRDS) (Pétron et
11 al., 2012; Farrell et al., 2013) and open path spectroscopy (Sun et al., 2014) are becoming more
12 common. Surface data were collected for the *GOSAT COMEX Experiment* by the AMOG
13 (AutoMOBILE trace Gas) Surveyor (Leifer et al., 2014). AMOG Surveyor is a commuter car
14 (Versa SP, Nissan, Japan) that is modified for mobile high-speed, high-spatial resolution
15 observations of meteorology (winds, temperature, and pressure), gases (greenhouse and other
16 trace), and remote sensing parameters (Fig. S2).



17

18

19 **Figure S2.** (a) AMOG Surveyor in the Transverse Coastal Range (1300 m) – San Joaquin Valley
 20 in background. (b) Cockpit view of gauges, security video, rear video, real-time data display. V_A ,
 21 V_{FB} , V_{RB} , V_I – voltages for alternator, front battery, rear battery, inverter. T_I , T_O , T_W – temperatures
 22 for inverter, engine oil, and radiator water. P_T , P_O , P_W , P_S , P_C , P_R – pressures for tires, oil, water
 23 suspension, compressor, and regulated air for chemical scrubbers. (c) AMOG Surveyor in Sierra
 24 Nevada Mountains, roof package labeled.

25 Analyzers: AMOG Surveyor draws air down two ½” PFA Teflon sample lines from 5 and 3 m
 26 above ground into a configurable range of gas analyzers by a high flow (30 cfm) vacuum pump
 27 (Edwards, GVSP30). The higher sample line connects to several analyzers including a Fast-flow,
 28 enhanced performance Greenhouse Gas Analyzer (FGGA), which uses Integrated Cavity Off-
 29 Axis Spectrometer-Cavity Enhanced Absorption Spectroscopy (ICOAS-CEAS) and measures
 30 carbon dioxide, CO_2 , methane, CH_4 , and water vapor, H_2O , at up to 10 Hz (Model 911-0010, Los
 31 Gatos Research, Inc., Mountain View, CA). AMOG also measures carbonyl sulfide (COS) and
 32 carbon monoxide (CO) with an ICOAS-CRDS analyzer (Model 907-0028, Los Gatos Research,
 33 Inc., Mountain View, CA). An additional sample line collects feeds an ICOAS-CRDS that
 34 measure ammonia (NH_3) and hydrogen sulfide (H_2S). Also, three chemiluminescence trace gas

35 analyzers measure nitric oxide (NO) and nitrogen oxides (NO_x) at 0.1 Hz at 25 ppt accuracy
36 (42TL, ThermoFischer Scientific, Waltham, MA), and ozone (O₃) at 0.25 Hz at 1 ppb accuracy
37 (42C, ThermoFischer Scientific, Waltham, MA), and sulfur dioxide (SO₂) at 0.1 Hz at 1 ppb
38 accuracy (450C, ThermoFischer Scientific, Waltham, MA). The FGGA is calibrated with an air
39 calibration standard for greenhouse gases (CH₄: 1.981 ppmv; CO₂: 404 ppmv; balance ultrapure
40 air). The 450C can achieve 50 ppt accuracy by hourly zero gas measurements using chemically
41 sparged air (Type CI, Cameron Great Lakes, PA).

42

43 Meteorology: A sonic anemometer (VMT700, Vaisala, Finland) mounted 1.4 m above the roof
44 measures two-dimensional winds. Recent science AMOG system improvements beyond (2014)
45 include a high speed thermocouple (50416-T, Cooper-Atkins, CT) and a high accuracy (0.2 hPa)
46 pressure sensor (61320V RM Young Co., MI), connected by a stainless steel line into a roof
47 passive radiation shield (7710, Davis Instruments, CA) to reduce dynamic pressure effects. The
48 radiation shield also includes a Type T thermocouple (Omega, CT) digitized at 0.03°C resolution
49 (CB-7018, Measurement Computing, MA). A solar insolation sensor is digitized at 16 bit and 1
50 Hz (CB-7017, Measurement Computing, MA). Two (redundant) Global Navigation Satellite
51 Systems (19X HVS, Garmin, KS) that use the GLONASS, GPS, Galileo, and QZSS satellites
52 provide position information at 10 Hz.

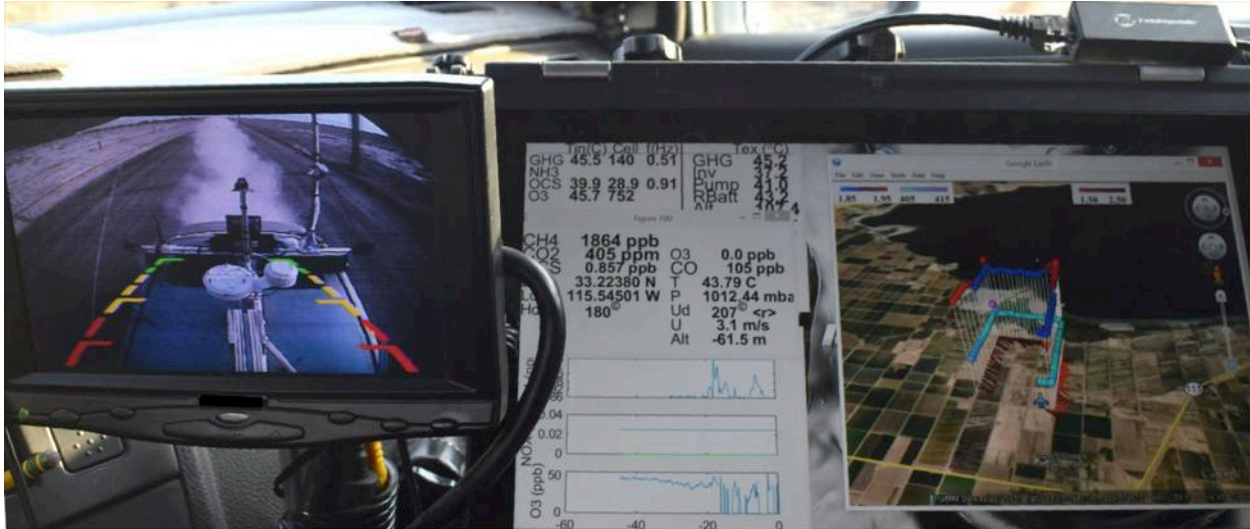
53

54 Vehicle Power: To support the science package (~1.8 kW), with clean DC and AC power,
55 AMOG has a 3.3 kW alternator (Nations Alternator, Cape Girardeau, MO), with a 2.7 kW
56 inverter (2810M, Outback Power, Arlington, OR), and a dual voltage conversion 2.4kW
57 uninterruptible power supply (Tripp Lite SU3000RTXL3U) backed by three, deep cycle gel
58 batteries for a total of 250 Amp-hours (Lifeline Batteries, WI; 6FM100H, Vision, MO; PVX-
59 1040T, Sun Xtender, CA) with active isolation (Dual Rectifier Isolator, Stolper International,
60 Inc., San Diego, CA). The 100 A-hr batteries and inverter are mounted in the cabin floor center
61 to improve stability. The DC system includes a 1-farad capacitor to stabilize against surges.

62

63 AMOG Surveyor weighs ~1 ton above stock, with significant safety implications, which were
64 addressed by enhancements to handling, suspension, and braking. Specifically, front drilled and
65 slotted ceramic brakes (F2473, Black Hart). Suspension modifications include rear airbag

66 suspension (NV-NINV-RBK, X2 Industries, AZ), adjustable rear truck shocks (for a Ford F-
67 150), performance coil-over front struts (TSC123, Tanabe, Japan), strut tower bar, sway bar, and
68 ladder brace.



69
70 **Figure S3.** AMOG Surveyor cockpit view showing real-time display (right) and rear camera
71 view in the Salton Sea, CA. Methane (CH_4) carbon dioxide (CO_2), and wind speed (U) and
72 direction (U_d) are shown in the Google Earth visualization window. Rolling display (lower left)
73 shows CH_4 , nitrogen oxides (NO_x) and ozone (O_3). Diagnostics window (upper left) shows cell
74 pressures and temperatures and key temperatures.

75 Data Handling and Integration: A touchscreen tablet (SpectreX360, HP) logs data
76 asynchronously from instruments and sensors through several serial Ethernet servers (5450
77 NPort, Moxa, Brea, CA) and industrial switches (EDS205, Moxa, Brea, CA). Logged data are
78 mirrored to a SSD LAN drive in AMOG. Acquisition time is identified to ~30 milliseconds from
79 the position of the data in the serial server buffer queues.

80
81 Custom software integrates the data streams and creates real time visualizations of multiple
82 parameters in the Google Earth environment to enable adaptive surveying (Thompson et al.,
83 2015). In adaptive surveying, the survey route is modified based on real time environmental
84 conditions (winds, new/unexpected sources, etc.). GoogleEarth visualizations are displayed on
85 one to several computers in AMOG Surveyor (**Fig. S3**) and remotely through cloud mirroring.
86 Viewing algorithms automatically follow the vehicle, rotated to display wind vectors, and adjust
87 the view altitude based on vehicle velocity. Algorithms minimize track overlap confusion
88 through selective use of transparency, i.e., when AMOG Surveyor returns on the same course, or

89 loops around. Rolling history displays of gas concentrations are useful for identifying recently
90 transected plumes. Other windows display AMOG Surveyor and analyzer diagnostics, and real
91 time analyzer gas and meteorology values.

92

93 **S2.2. Airborne - AJAX**

94 Airborne *in situ* data were collected by AJAX (Alpha Jet Atmospheric eXperiment), operated
95 from NASA Ames Research Center (ARC) at Moffett Field, CA. The alpha jet aircraft, which
96 has been modified for science missions, measures carbon dioxide and methane (Picarro Inc.,
97 model G2301-m), ozone (2B Technologies Inc., model 205), formaldehyde (COmpact
98 Formaldehyde Fluorescence Experiment, COFFEE), and meteorological parameters including
99 3D winds (Meteorological Measurement System, MMS) from two externally-mounted wing
100 pods (**Fig. S4**). The greenhouse instrument was calibrated using whole-air (National Oceanic and
101 Atmospheric Administration) standards before and after aircraft deployment. The ozone sensor is
102 frequently calibrated to a NIST- traceable standard. Further details on the aircraft and
103 instrumentation are reported by Hamill et al. (2015); Tanaka et al. (2016) and Yates et al. (2013).



104

105 **Figure S4.** AJAX photo. Courtesy Warren Gore, NASA Ames Research Center.

106 The Alpha Jet is owned by H211, LLC, a collaborative partner with NASA. It is a tactical strike
107 fighter developed by Dassault-Breguet and Dornier through a German-French NATO
108 collaboration. Dassault concurrently developed a trainer version of the Alpha Jet that is still in
109 service with the French Air Force. Carrying a crew of two, it has a length of 12.2 m, a wingspan

110 of 9.2 m, and a height of 4.2 m. Its empty weight is 3540 kg and a maximum takeoff weight of
111 8000 kg. It has a ceiling of 15,545 m, speed of 280 – 930 km/hr, and a range of approximately
112 1930 km with full fuel.

113

114 The Alpha Jet stationed at NASA Ames – Moffett Field is operated in accordance with an FAA
115 Experimental Certificate of Airworthiness. It has a 2 – 2.5 hr flight duration, permitting up to
116 two missions per day with appropriate crew changes. Three highly experienced H211 pilots are
117 FAA Type Certificated to fly the Alpha Jet, and science test flights began in September 2010.
118 Following a complete avionics update and installation of the NASA-specified payload
119 management and control system in early 2009, the Alpha has proven extremely robust and
120 reliable. Its fleet safety record as a twin-engine, all weather jet is excellent, and its modern
121 Snecma engines produce a noise signature equivalent to current generation Stage III noise
122 compliant turbofan aircraft.

123

124 H211 has provided significant upgrades to the aircraft to support scientific studies. Extensive
125 wiring and cabling provisions have been installed to both wing pod locations, as well as the
126 centerline pod, to allow for distribution of 120 and 26 volt AC and 28 volt DC to each wing pod,
127 as well as additional 120 volt AC and 28 volt DC service to the centerline pod. Redundant
128 heavy-duty Ethernet cables have been provided from the wing pods to the centerline pod and
129 backseat control console. An operator interface panel has been installed in the rear cockpit to
130 allow power on/off/failure interface to each scientific instrument. Additionally, the pilot has a
131 payload master power switch that can remove all electrical power from the NASA payloads in
132 the event an abnormal electrical condition is encountered.

133

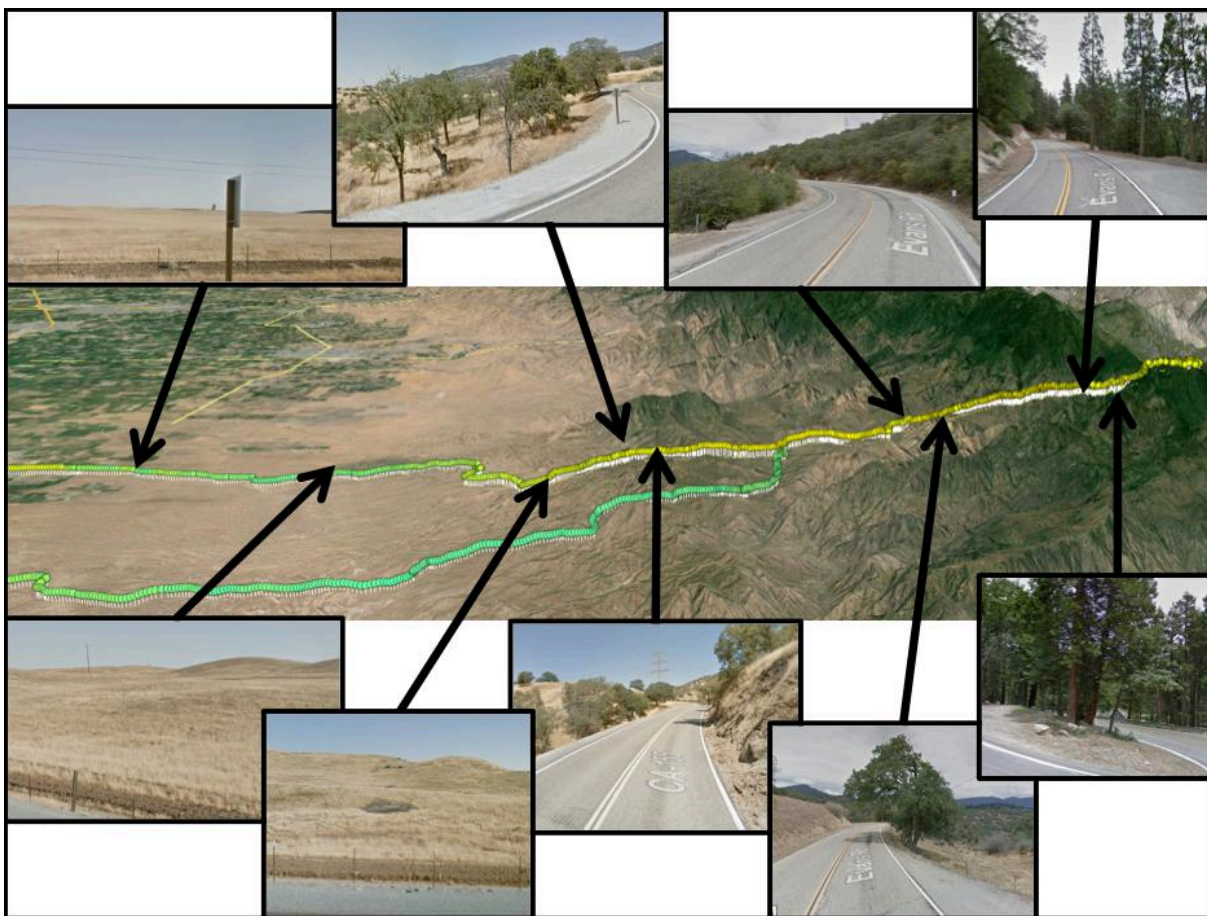
134 Multiple redundant Garmin G600/G530/G430/G696 systems record and display position,
135 attitude, heading, altitude, true airspeed, groundspeed, true air temperature, wind speed, wind
136 direction, and a wide variety of additional data through dual digital air data computers. This
137 information is recorded for science use. A digital autopilot system allows highly accurate
138 heading and track control via GPS steering, plus precise altitude control during air sampling
139 missions. AJAX flights can also be followed in real-time using the NASA Airborne Science
140 Mission Tool Suite.

141
142 Two wing-mounted pods have been modified by NASA-ARC to carry instrumentation, with
143 three down-looking window ports available on each pod. Each wing pod has an approximate
144 available volume of 0.1 cubic meter, with a maximum payload weight of 136 kg. The centerline
145 pod has two payload areas of approximately 86.4 x 25.4 x 30.5 cm and 68.6 x 16.5 x 25.4 cm,
146 carrying combined payloads up to 136 kg total.

147

148 **S4. Upwind Profile**

149 An upwind pre-survey east-west transect was conducted by AMOG from Delano (~70 m) on the
150 floor of the San Joaquin Valley to Alta Sierra (~1750 m) on the ridge of the Greenhorne
151 Mountains in the Sierra Nevada Mountain Range (Fig. S5). This survey passed through a range
152 of surface topography and vegetation and canopy types. Example Google Maps “street images”
153 show variation from flat grasslands to rolling grass covered hills, to scattered low oak trees, to at
154 the highest altitudes, dense, tall pine forests. The road shifts from an initial gradual rise while
155 following a primarily straight and gently curved pathway, to steeper climbs cut into steep slopes
156 with sharp curves, and even hairpin curves.

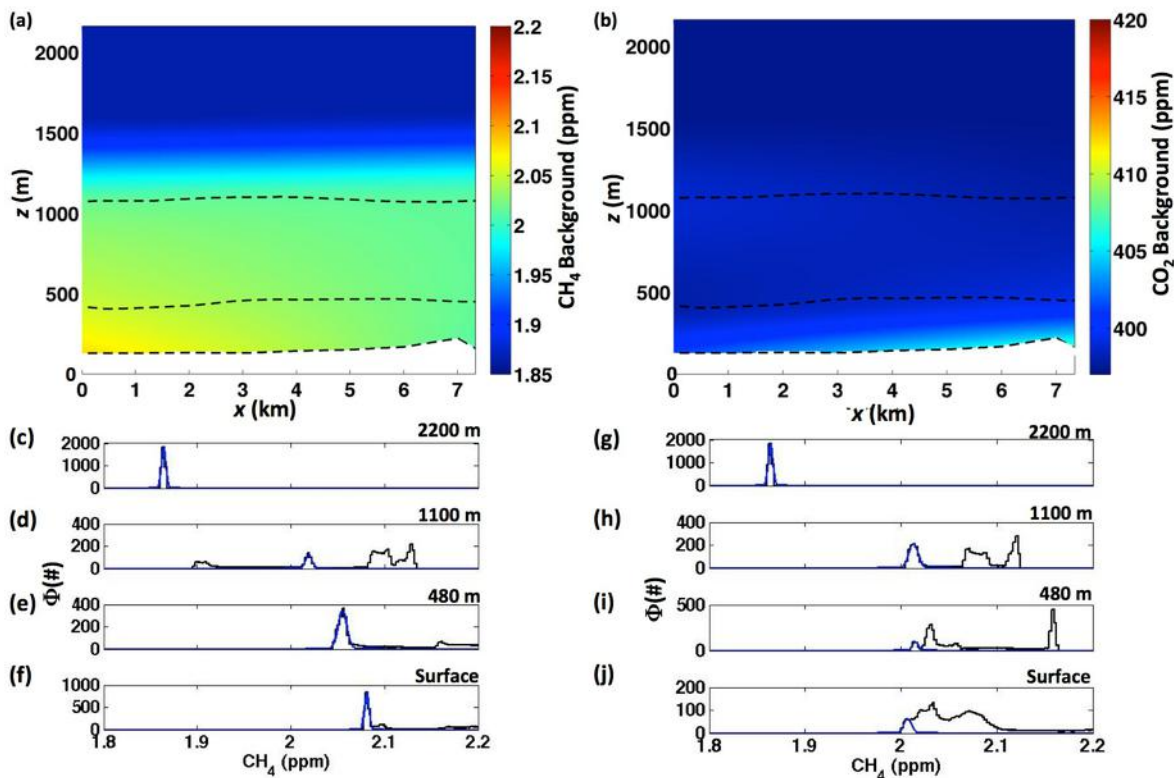


157
 158 **Figure S5** – Sierra Nevada Mountain Range vertical profile, and Google maps street images
 159 showing changing terrain.

160 **S5. Derivation of the background data curtain**

161 The background data plane (Fig. S6) for transect $\gamma-\gamma'$ (Fig. 7) showed a trend of increasing CH_4
 162 towards the west, rising more than ~ 25 ppb, at both the surface and at 480 m altitude. In contrast,
 163 background CO_2 across the data curtain was quite uniform.

164
 165 Anomaly concentration was relative to the background concentration curtain (Fig. S6a & 6b) and
 166 was derived by estimating the background concentration at each transect altitude from fitting a
 167 Gaussian to the background occurrence concentration distribution and using the distribution peak
 168 as the background concentration (Fig. S6c-S6f). The methodology is described in Sect. 2.5.



169
 170 **Figure S6** – Background (a) methane (CH₄) and (b) carbon dioxide (CO₂) data curtain. Dashed
 171 line shows data altitudes. (c-f) CH₄ and (g-j) CO₂, data probability distributions (Φ).

172 References

- 173 Farrell, P., Leifer, I., Culling, D., 2013. Transcontinental methane measurements: Part 1. A
 174 mobile surface platform for source investigations. *Atmospheric Environment* 74, 422-431,
 175 doi:10.1016/j.atmosenv.2013.02.014
- 176 Hamill, P., Iraci, L.T., Yates, E.L., Gore, W., Bui, T.P., Tanaka, T., Loewenstein, M., 2015. A
 177 new instrumented airborne platform for atmospheric research. *Bulletin of the American*
 178 *Meteorological Society* 97, doi:10.1175/BAMS-D-14-00241.1
- 179 Leifer, I., Melton, C., Manish, G., Leen, B., 2014. Mobile monitoring of methane leakage. *Gases*
 180 *and Instrumentation* July/August 2014, 20-24,
- 181 Pétron, G., Frost, G., Miller, B.R., Hirsch, A.I., Montzka, S.A., Karion, A., Trainer, M.,
 182 Sweeney, C., Andrews, A.E., Miller, L., Kofler, J., Bar-Ilan, A., Dlugokencky, E.J., Patrick,
 183 L., Moore, C.T.J., Ryerson, T.B., Siso, C., Kolodzey, W., Lang, P.M., Conway, T., Novelli,
 184 P., Masarie, K., Hall, B., Guenther, D., Kitzis, D., Miller, J., Welsh, D., Wolfe, D., Neff, W.,
 185 Tans, P., 2012. Hydrocarbon emissions characterization in the Colorado Front Range: A pilot
 186 study. *J. Geophys. Res.* 117, D04304, doi:10.1029/2011jd016360
- 187 Sun, K., Tao, L., Miller, D.J., Khan, A.M., Zondlo, M.A., 2014. On-road ammonia emissions
 188 characterized by mobile, open-path measurements. *Environmental Science & Technology* 48,
 189 3943-3950, doi:10.1021/es4047704 |
- 190 Tanaka, T., Yates, E., Iraci, L.T., Johnson, M.S., Gore, W., Tadi, J.M., Loewenstein, M., Kuze,
 191 A., Frankenberg, C., Butz, A., Yoshida, Y., 2016. Two-year comparison of airborne

192 measurements of CO₂ and CH₄ with GOSAT at Railroad Valley,
193 Nevada. IEEE Transactions on Geoscience and Remote Sensing 54, 4367-4375,
194 doi:10.1109/TGRS.2016.2539973

195 Thompson, D., Leifer, I., Bovensman, H., Eastwood, M., Fladeland, M., Frankenberg, C.,
196 Gerilowski, K., Green, R., Krautwurst, S., Krings, T., Luna, B., Thorpe, A.K., 2015. Real-
197 time remote detection and measurement for airborne imaging spectroscopy: A case study
198 with methane. Atmospheric Measurement Techniques 8, 1-46, doi:10.5194/amtd-8-1-2015

199 Yates, E.L., Iraci, L.T., Roby, M.C., Pierce, R.B., Johnson, M.S., Reddy, P.J., Tadić, J.M.,
200 Loewenstein, M., Gore, W., 2013. Airborne observations and modeling of springtime
201 stratosphere-to-troposphere transport over California. Atmos. Chem. Phys. 13, 12481-12494,
202 doi:10.5194/acp-13-12481-2013

203